Kinetik: Game Technology, Information System, Computer Network, Computing, Electronics, and Control
Journal homepage: http://kinetik.umm.ac.id
ISSN: 2503-2267
Vol. 11, No. 2, May, Pp. 237-248

Comparative performance analysis of nutrient and pH control in hydroponic systems using coupled and decoupled methods

Ina Rahmawati Putri[1], Bambang Siswojo[1], Mochammad Rusli[1]
Electrical Engineering Department, Universitas Brawijaya Malang, Indonesia [1]

Article Info
Keywords:
NFT Hydroponics, Decouple, Couple, PID, MIMO

Article history:
Received: September 22, 2025
Accepted: December 15, 2025
Published: May 01, 2026

Cite:
I. R. Putri, B. Siswojo, and M. Rusli, "Comparative Performance Analysis of Nutrient and pH Control in Hydroponic Systems Using Coupled and Decoupled Methods", *KINETIK*, vol. 11, no. 2, May. 2026.
https://doi.org/10.22219/kinetik.v11i2.2504

*Corresponding author.
Mochammad Rusli
E-mail address:
rusli@ub.ac.id

Abstract
pH and TDS are critical parameters in hydroponic systems that directly influence plant growth. This research develops an automatic control system for nutrient solution and pH regulation in hydroponic cultivation using a PID controller implemented with both coupled and decoupled methods. The aim of the research is to evaluate the performance differences between these two control approaches and to contribute to the development of more accurate and adaptive strategies for maintaining nutrient solution quality. Lettuce plants were used as test subjects with target conditions of 550 ppm TDS and pH 6.5. The research was conducted through MATLAB simulations and hardware implementation to assess system performance. The simulation results indicated that the decoupled method provides superior performance, achieving a pH rise time of 6.04 s, a settling time of 31.24 s, an overshoot of 9.5%, and zero steady-state error. The TDS response exhibits a rise time of 84.97 s, a settling time of 161.67 s, zero overshoot, and zero steady-state error. Hardware implementation demonstrates similar trends, with a pH rise time of 8.34 s, a settling time of 11 s, zero overshoot, and a steady-state error of 0.90%. The TDS response shows a rise time of 30.7 s, a settling time of 36 s, an overshoot of 4.36%, and a steady-state error of 0.60%. In contrast, the coupled method produces slower responses, longer settling times, and higher steady-state errors. Overall, the decoupled method proves to be more effective and responsive in maintaining pH and nutrient stability, demonstrating strong potential for application in smart agriculture systems.

1. Introduction

Indonesia is a tropical country with warm and humid conditions, characterized by air temperatures of 22.8–32.2°C and an average relative humidity of 77%, which naturally supports the growth of tropical crops [1]. However, population growth and rapid urbanization have increased pressure on urban areas, resulting in the conversion of agricultural land into residential zones and infrastructure. Consequently, the availability of productive land for conventional farming has declined, particularly in peri-urban regions that are highly susceptible to land-use change. This reduction in cultivation capacity highlights the need for innovative farming systems that can operate efficiently even in limited spaces [2]. To address this challenge, alternative cultivation methods such as hydroponics offer a promising solution, as they maximize land and water efficiency while enabling the production of high-quality agricultural products [3].

One of the main challenges in hydroponic systems is maintaining stable pH and Total Dissolved Solids (TDS) levels in the nutrient solution, as both parameters directly affect nutrient availability and plant growth [4]. Imbalances in pH and TDS values can cause physiological disorders, reduced yield, and even plant death. pH deviations greater than ±0.5 from the optimal value can inhibit micronutrient absorption, while TDS fluctuations exceeding ±50 ppm may reduce plant growth rates by 10–15% [5]. Manual monitoring and adjustment of these parameters are considered inefficient and prone to error, especially for novice or small-scale farmers. Therefore, an automated system capable of controlling pH and TDS in real time with high precision is needed. The digitization of hydroponic systems through the integration of sensors and microcontrollers is considered effective in increasing efficiency, reducing the risk of crop failure, and supporting the implementation of precision agriculture [6], [7], [8]. Deviations in pH or TDS can reduce nutrient absorption efficiency and lead to suboptimal plant development. Although various automatic control approaches have been proposed, most practical hydroponic systems still rely on conventional control strategies that treat pH and TDS as independent variables. However, the main unresolved issue lies in the fact that pH and TDS form a strongly coupled multivariable system, which is not adequately addressed by independent control strategies.

Research [9] developed an automatic hydroponic system based on an Adaptive Network-Based Fuzzy Inference System (ANFIS) integrated with Internet of Things (IoT) technology to monitor and control pH and plant nutrients in real time. The system was able to maintain pH and Electrical Conductivity (EC) in nutrient solutions within the optimal range of 5.5–6.5, with fast response, high accuracy, and good stability. Despite its strong performance, the ANFIS approach still has limitations in handling multivariable systems with complex interactions, such as the coupling between pH and EC. In addition, the effectiveness of the model is highly dependent on the quality of the training data, requiring representative and error-free datasets.

Research [10] investigated a nutrient control system in Nutrient Film Technique (NFT) hydroponics using the Convolutional Neural Network (CNN) method. The study reported high accuracy with a low error rate: the pH sensor achieved 99.02% accuracy and the TDS sensor achieved 96.65%, while the CNN model showed good performance with an MSE value of 0.0057 and an RMSE of 0.075. However, this research was conducted in a controlled environment and did not consider variations in real conditions such as changes in temperature, humidity, and other environmental factors that may influence plant growth. In addition, the CNN method has several limitations, including high computational requirements, a time-consuming training process, and less-than-optimal performance in handling multivariable systems with complex interactions [11].

Control in multivariable systems such as pH and TDS generally experience cross-interactions between variables that can cause instability and slow down system response. Research [12] shows that MIMO systems exhibit significant inter-loop effects, meaning that changes in one variable can influence the dynamics of other variables. This condition underscores the need for a control approach capable of reducing the impact of these cross-interactions. To address the complexity of the interactions between pH and Total Dissolved Solids (TDS), the decoupling method is employed. This method separates the influence between variables so that each variable can be regulated independently [13]. Once the interactions are successfully decoupled, control is implemented by applying PID (Proportional–Integral–Derivative) controllers to each individual loop. PID was selected due to its ability to provide fast, stable, and effective responses in maintaining pH and nutrient concentrations within the optimal range [14]. The effectiveness of PID control is highly dependent on the accuracy of its parameter settings. Therefore, the Ziegler–Nichols Type 1 method was chosen for PID tuning, as this method is considered simple and consistent in providing suitable initial parameters for process systems, thereby supporting the achievement of stable and responsive control performance [15].

The novelty lies in the direct comparative validation between coupled and decoupled PID controllers in hydroponic systems through simulation and hardware implementation. The developed control system regulates the delivery of nutrient solution and pH to hydroponic plants using PID with the decoupled method to reduce the cross-coupling effect between pH and TDS and is then experimentally compared with the coupled method without interaction separation. The objective of this research is to determine whether PID controllers with the decoupled method are capable of achieving faster settling times and lower steady-state errors in NFT hydroponic nutrient regulation compared to the coupled method. This research focuses on analyzing real multivariable control system dynamicsresponses, rather than data-based prediction or classification. In the experiment, a DFRobot Gravity: Analog TDS sensor was used to measure nutrient concentration, an Electrode Probe pH-4502C sensor was used as a pH detector, and an Arduino Uno was used as the main controller to operate three peristaltic pumps in real time. Observations were conducted on lettuce plants with TDS requirements of 550 ppm and pH 6.5.

1.1 Comparison with Previous Methods

Technological developments in hydroponic systems have led to various control methods to maintain stable pH and Total Dissolved Solids (TDS) levels. Machine learning-based approaches such as the Adaptive Network-based Fuzzy Inference System (ANFIS) and the Convolutional Neural Network (CNN) show good performance in monitoring and predicting nutrient parameters; however, they have limitations in terms of computational requirements and dependence on training data and are less effective when applied to multivariable systems with strong interactions between pH and TDS. On the other hand, coupled methods are simple and easy to implement on microcontroller devices, but they are unable to handle cross-interactions, thereby reducing the stability of the control system.

To highlight the differences in the characteristics of each method, Table 1 provides a summary of control methods developed in previous studies compared with the methods applied in this research.

Table 1. Comparison of Hydroponic Control Methods in Previous Studies and This Research

Method	Model Complexity	Ability to Manage Interactions	Hardware Implementation Suitability	Advantages	Weakness
ANFIS	High	Currently	Currently	Adaptive and accurate	Depends on the quality of training data; less effective for MIMO systems
CNN	Very high	Low	Low	High prediction accuracy	Not suitable for real-time control; heavy computation

Method	Model Complexity	Ability to Manage Interactions	Hardware Implementation Suitability	Advantages	Weakness
Coupled	Low	Poor	Good	Simple and easy to use	Affected by cross-interactions, resulting in instability
Decoupled	Currently	Very good	Very good	Stable, fast, and robust against crosstalk	Initial process modeling required for the decoupler design

Based on Table 1, the use of the decoupled method in this research provides significant advantages over previous methods. This method is able to reduce the influence of cross-coupling between pH and TDS, allowing each variable to be controlled more precisely and stably. In addition, the computational requirements remain low, making it highly feasible for hardware implementation.

2. Research Method

2.1 Plant Modeling

This process modeling represents the physical system in the form of a mathematical model that describes the relationship between inputs and outputs, allowing the dynamic characteristics of the plant to be analyzed and used as a basis for control-system design and evaluation [16]. In this research, four plants are considered: a pH plant, a TDS plant, a pH–TDS plant (representing the effect of pH on TDS changes), and a TDS–pH plant (representing the effect of TDS on pH changes). The determination of these four plant models is based on the working principle of the MIMO control system, which requires interrelated variables between the input and output loops. Based on these four datasets, plant modeling was carried out to obtain transfer functions using the First-Order Plus Dead Time (FOPDT) method, as expressed in Equations 1 to 4.

$$H_{(11)} = \frac{0.026}{15s+1}e^{-5s} \tag{1}$$

$$H_{(12)} = \frac{0.003}{15s+1}e^{-4s} \tag{2}$$

$$H_{(21)} = \frac{0.257}{17.7s+1}e^{-1,3s} \tag{3}$$

$$H_{(22)} = \frac{3.71}{5.7s+1}e^{-8.8s} \tag{4}$$

2.2 Decouple Control

Decoupling control is a method in Multi-Input Multi-Output (MIMO) control systems designed to reduce or eliminate the effects of interaction between control loops so that each loop can operate independently and be more easily controlled. Decoupling is achieved by designing a compensator (decoupler) that corrects cross-channel interference so that each input affects only one primary output [17], [18], [19].

The development of a decoupled PID-based control method was applied to improve the accuracy of pH and TDS control in NFT hydroponic systems [20]. It began with modeling the process dynamics using the FOPDT method to obtain the transfer functions of each variable and the cross-interactions between control channels. The transfer function model was then used in the design of a decoupler that reduces cross-talk between the pH and TDS loops, allowing both variables to be controlled more independently [21]. After the interaction effects were successfully reduced, each loop was controlled using a PID controller that was tuned separately to achieve a fast, stable, and accurate dynamic response. The integration of the decoupler and PID controller resulted in a control structure capable of maintaining pH and TDS stability simultaneously, ensuring that the nutrient regulation process in the NFT hydroponic system could take place more consistently and measurably.

The block diagram of the MIMO control system with decoupling is shown in Figure 1. It consists of several transfer function blocks, namely $H_{11}(s)$, which represents the transfer function of pH, and $H_{22}(s)$, which represents the transfer function of TDS. The diagram also shows cross-interaction through $H_{21}(s)$ and $H_{12}(s)$, indicating a cross relationship between the two variables. Block $H_{21}(s)$ illustrates the effect of the pH control signal on TDS, while block $H_{12}(s)$

illustrates the effect of the TDS control signal on pH. This cross-interaction has the potential to cause instability or inaccurate control if not handled properly. To overcome this, the interaction is compensated by adding decoupler blocks $D_1(s)$ and $D_2(s)$.

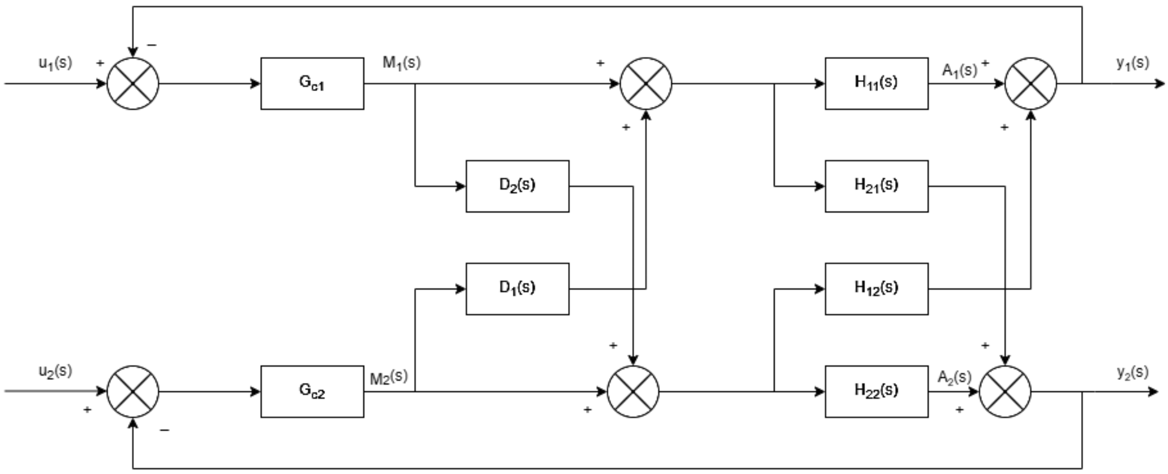

Figure 1. Decouple Control System Block Diagram

Decoupler blocks are designed to eliminate the effects caused by cross-interaction blocks, ensuring that each control variable is not affected by changes in the manipulated variable in the other loop. The decoupling formulas are expressed in Equations 5 and 6 [22].

$$D1(s) = -\frac{H_{12}}{H_{11}} = -\frac{0.003}{0.026} = -0.11 \tag{5}$$

$$D2(s) = -\frac{H_{21}}{H_{22}} = -\frac{0.257}{3.71} = -0.069 \tag{6}$$

The relationship between each control variable and manipulated variable in a decoupling compensated control system can be written as follows:

$$\frac{A_1(s)}{M_1(s)} = H_{11}(s) + D_2(s)H_{12}(s) \tag{7}$$

$$\frac{A_2(s)}{M_2(s)} = H_{22}(s) + D_1(s)H_{21}(s) \tag{8}$$

From Equations 7 and 8, in the decoupled system, each manipulated variable affects the control variable through parallel paths. If Equation 5 is substituted into Equation 7 and Equation 6 is substituted into Equation 8, the resulting expressions are obtained.

$$\frac{A_1(s)}{M_1(s)} = [D_1(s) - \frac{H_{21}(s)H_{12}(s)}{H_{22}}] \tag{9}$$

$$\frac{A_2(s)}{M_2(s)} = [D_2(s) - \frac{H_{12}(s)H_{21}(s)}{H_{11}}] \tag{10}$$

Equations 9 and 10 show that, after the decoupling process, the cross-influence between pH and TDS has been compensated through a combination of cross-transfer functions and decouplers. The end result is a control path that behaves like a SISO system, where each manipulated variable primarily affects its corresponding controlled variable.

2.3 PID

PID (Proportional–Integral–Derivative) is a feedback control strategy that is widely used in control systems. PID works by calculating the error between the desired value (setpoint) and the actual value (output) of a system and then applying three control actions: proportional gain (K_p), which affects the response speed; integral gain (K_i), which eliminates steady-state error; and derivative gain (K_d), which improves stability and reduces overshoot [23]. The combination of these three actions allows PID to maintain stability and achieve optimal response in various dynamic systems. Equation 11 presents the PID controller formula.\

$$u(t) = K_P e(t) + K_i \int_0^t e(t)dt + K_d \frac{de(t)}{dt} \tag{11}$$

2.4 Couple Control System

A coupled system is a type of system with more than one variable. In such systems, variables interact with each other so that changes in one variable not only affect the main output but also impact other variables in the system. This characteristic is commonly found in MIMO systems [24]. MIMO refers to a control system that involves multiple variables that are controlled and manipulated simultaneously. Such systems exhibit strong cross-coupling between variables, meaning that a change in one input can produce a response in more than one output. This interrelated multivariable dynamics implies that, in a coupled system, each input change not only affects its own control loop but also influences other connected loops [25].

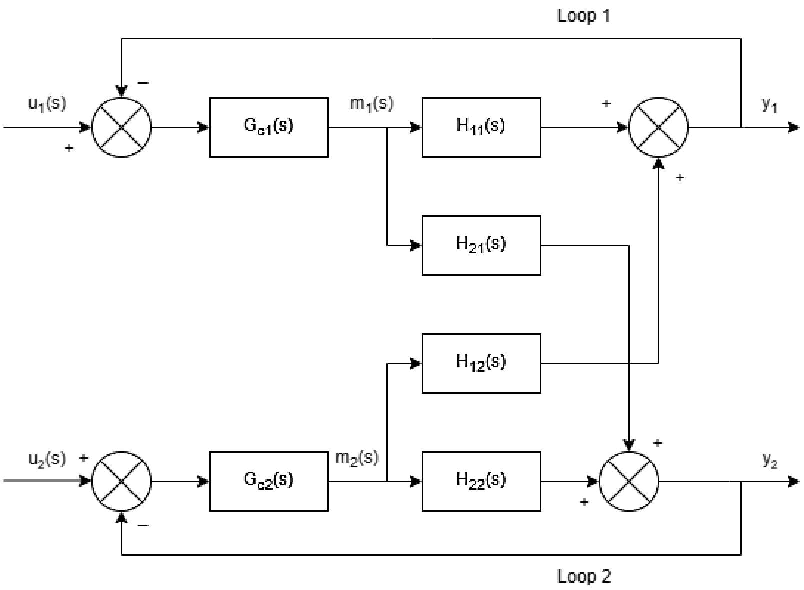

Figure 2. MIMO Control System Block Diagram

Figure 2 shows a MIMO control block diagram that illustrates the signal flow between the controller and the plant in a two-variable system. Controllers $G_{c1}(s)$ and $G_{c2}(s)$ function to generate control signals for each manipulated variable based on the error. Meanwhile, blocks $H_{11}(s)$ and $H_{21}(s)$ represent the main transfer functions of the plant for each process variable. The blocks $H_{12}(s)$ and $H_{22}(s)$ illustrate the cross-interaction between process variable 1 and 2, indicating that a change in one manipulated variable can affect the output of the other variable. Control of this coupled system is performed without using decoupling transfer function blocks such as $D_1(s)$ and $D_2(s)$, allowing all interactions between variables to occur naturally in the control loop. This approach aims to evaluate system performance under coupled control conditions and compare it with decoupled control to understand the extent to which interaction effects influence stability, dynamic response, and control accuracy in interconnected systems. Equations 12 and 13 describe the relationship between input and output signals in a MIMO system.

$$y_1(s) = H_{11}(s)m_1(s) + H_{12}(s)m_2(s) \tag{12}$$

$$y_2(s) = H_{21}(s)m_1(s) + H_{22}(s)m_2(s) \tag{13}$$

In Equation 12, the output $y_1(s)$ is influenced by two inputs, namely the contribution from the first manipulated variable through the transfer function $H_{11}(s)$ and the cross-influence from the second manipulated variable through the transfer function $H_{12}(s)$. Similarly, in Equation 13, the output $y_2(s)$ is a combination of the influence of the first manipulated variable modeled by $H_{21}(s)$ and the contribution of the second manipulated variable through $H_{22}(s)$. These two equations show that each output variable depends not only on the manipulated variable but is also affected by other variables in the system, thus confirming the existence of interaction or cross-coupling in the MIMO system.

2.5 Ziegler Nichols Type 1

The Ziegler–Nichols Type 1 method is one of the PID controller tuning techniques used to empirically determine the values of the K_p, K_i, and K_d parameters in a FOPDT system, with the objective of producing a fast and stable system response. The system receives input in the form of pH levels or reference nutrient levels (setpoints), which are compared with actual levels to produce an error signal. This signal is processed by the PID controller to generate a control signal that drives the peristaltic pump [26]. The determination of the PID parameters (K_p, K_i, K_d) was carried out using the Ziegler Nichols Type 1 step-response method, in which the dynamic response of the system under open-loop conditions was analyzed to obtain the process characteristics. The required process characteristics in this method include dead time (L), time constant (T), and process gain (K). The process gain (K) represents the magnitude of output change with respect to an input change and therefore strongly influences system sensitivity, response speed, and closed-loop stability. A gain that is too high may lead to oscillatory behavior or instability, whereas a gain that is too low results in a sluggish response. Thus, determining an appropriate gain value is essential to achieve a balance between fast response and stable system dynamics.

The gain is calculated based on the relationship between the change in process output (ΔY) and the change in input (ΔU) during the step-response test, as shown in Equation 14.

$$K = \frac{\Delta Y}{\Delta U} \tag{14}$$

The obtained values of K, T, and L were then used in Table 2 to determine the parameters K_p, K_i, and K_d according to the Ziegler–Nichols Type 1 tuning rules, ensuring that the resulting system response is stable and efficient.

Table 2. PID Ziegler Nichols Type 1

Controller Type	K_p	T_i	T_d	K_i	K_d
P	$\frac{T}{L}$	∞	0	∞	0
PI	$0.9\,\frac{T}{L}$	$\frac{L}{0.3}$	0	$\frac{K_p}{T_i}$	0
PID	$1.2\,\frac{T}{L}$	$2L$	$0.5\,L$	$\frac{K_p}{T_i}$	$K_p \times T_d$

3. Results and Discussion

3.1 Comparison of Couple and Decouple Simulations

The simulation in Figure 3 implements a MIMO system model for coupled pH and TDS control. The setpoints for pH and TDS are 6.5 and 550 ppm, respectively, and are represented in the simulation by step-input signal blocks. The signals from these setpoints are then compared with the feedback values from the sensor measurements to produce error signals. These error signals are processed by a PID controller to generate control signals that drive the actuator in the form of a peristaltic pump.

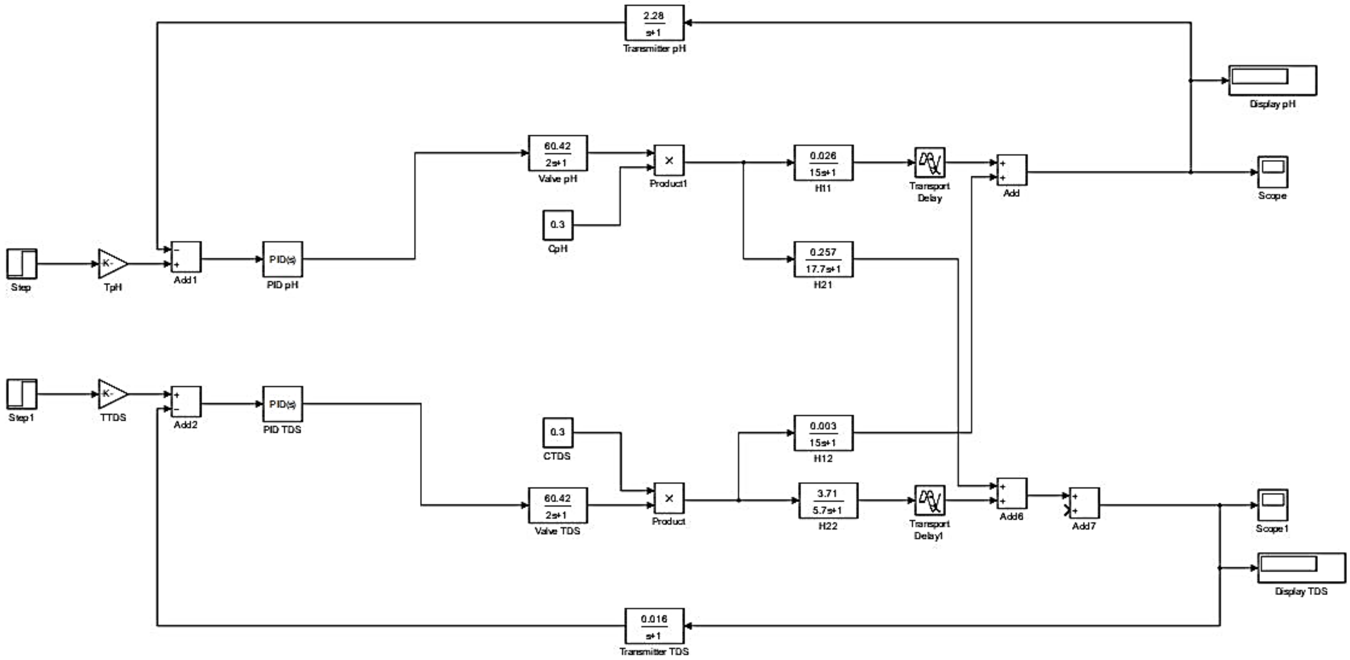

Figure 3. Couple Simulation

The simulation in Figure 4 implements the decoupling method for pH and TDS control. Blocks D_1 and D_2 serve to reduce cross-influence between variables, allowing each loop can respond more stably and approximate a Single Input Single Output (SISO) system.

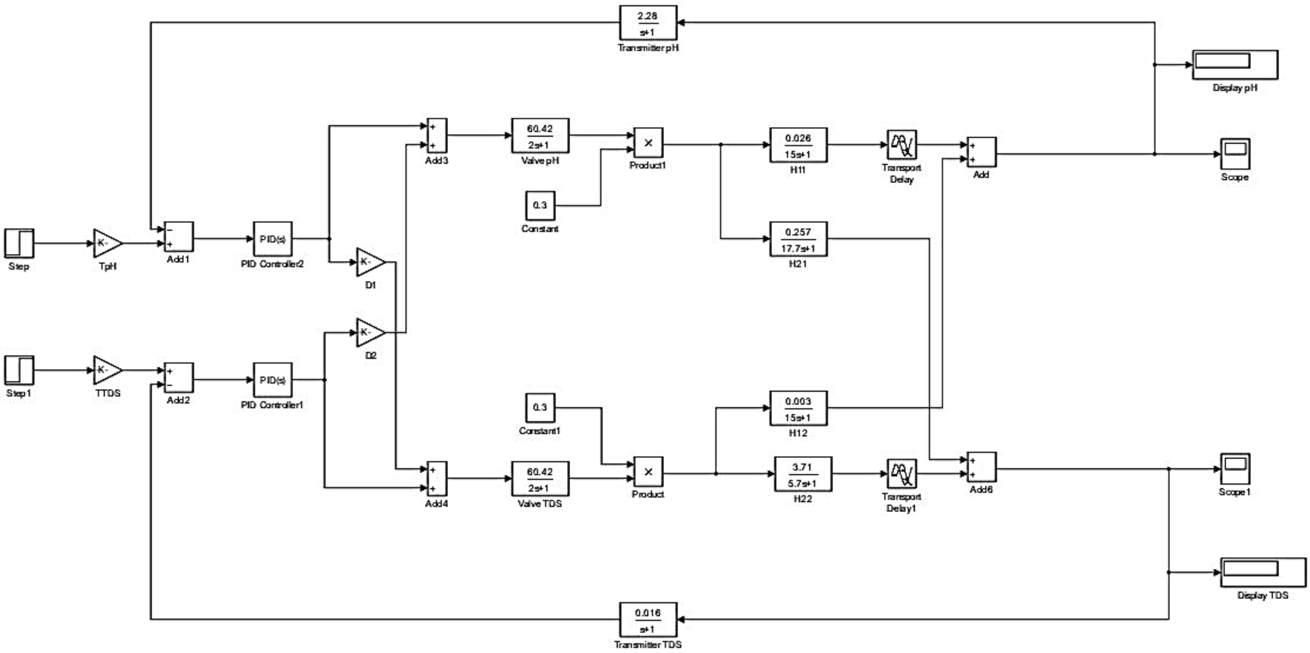

Figure 4. Decouple Simulation

The K_p, K_i, and K_d parameters in the coupled and decoupled methods were obtained from calculations using the Ziegler–Nichols Type 1 method, utilizing the process time constant (T) and death time (L) parameters resulting from the FOPDT model identification. The PID parameters are shown in Table 3.

Table 3. PID Parameter

Controller	PID Parameter		
	Kp	Ki	Kd
PH	3.6	0.36	9
TDS	0.7	0.03	3.08

The couple simulation results are shown in Figure 5 (a) as the pH system response, while Figure 5 (b) shows the TDS system response.

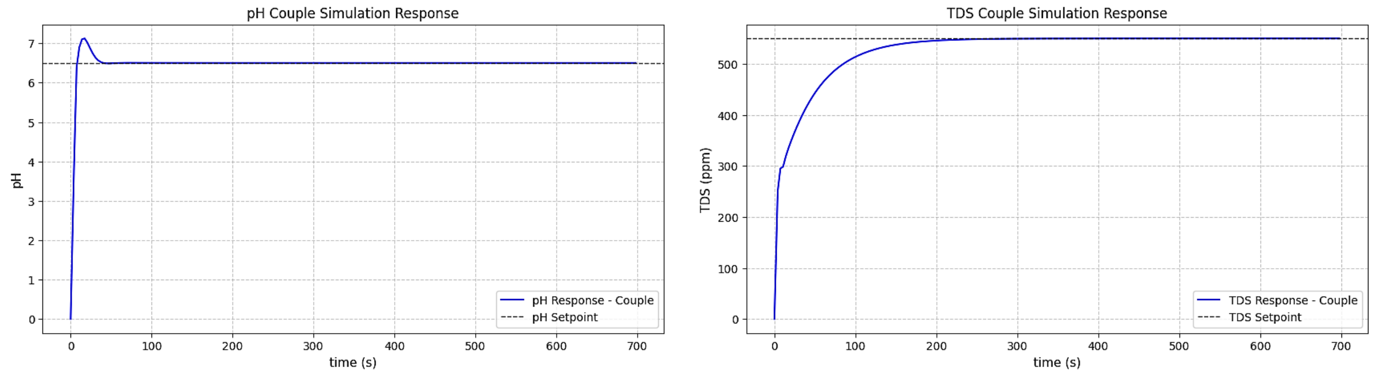

(a) (b)

Figure 5. Simulation Result: (a) PH System Response Couple, (b) TDS System Response Couple

The simulation test results obtained using the coupled response system method in Figure 5(a) show that the pH response has a rise time of 5.982 s, a settling time of 30.973 s, zero steady-state error, and an overshoot of 9.56%. Although the response appears fast and reaches steady state, the overshoot indicates an overly aggressive control action. This is consistent with MIMO system theory, where cross-coupling through the $H_{12}(s)$ path causes changes in the TDS variable to act as internal disturbances to the pH loop. When TDS changes, the pH controller must compensate for the disturbance even though it does not originate from the pH process, resulting in more aggressive transient dynamics. The TDS system response shown in Figure 5(b) has a rise time of 79.696 s, a settling time of 155.028 s, an overshoot of 0%, and a steady-state error of 0, indicating a relatively sluggish process in reaching a stable condition

The decoupled simulation results are shown in Figure 6 (a) as the pH system response, while Figure 6 (b) shows the TDS system response.

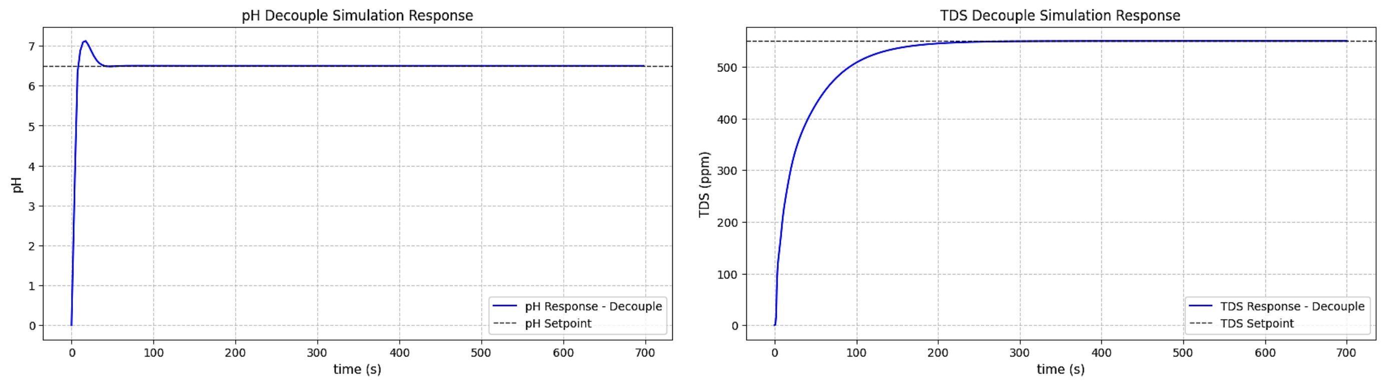

(a) (b)

Figure 6. Simulation Result: (a) PH System Response Decouple, (b) TDS System Response Decouple

The results of the simulation tests conducted using the decoupled method can be seen in Figure 6(a). The pH response has a rise time of 6.040 s, a settling time of 31.24 s, a smaller overshoot of 9.5%, and a steady-state error of 0. This system shows a fast and well-damped stability response. The response characteristics of this system are almost equivalent to those of the coupled method, but the response dynamics are now more predictable. This occurs because decoupling has compensated for the cross-influence of $H_{12}(s)$ and $H_{21}(s)$, so that the pH control signal is no longer affected by TDS-induced disturbances. This separation means that the addition of pH control solution does not cause significant changes in nutrient concentration, allowing the pH controller to operate according to its intrinsic loop dynamics. In Figure 6(b), the TDS response has a rise time of 84.97 s and a settling time of 161.67 s, showing slightly slower characteristics; however, the absence of cross-interference allows the controller to operate more stably, with 0% overshoot and zero steady-state error. This is in line with control theory, which states that decoupling reduces loop interaction and overall control load, allowing each loop to operate closer to SISO-like behaviour. Overall, these simulation results confirm that the decoupling strategy effectively suppresses inter-loop disturbances in the multivariable pH–TDS control system. By mitigating cross-coupling effects, the control structure improves response predictability and stability without increasing controller aggressiveness, thereby enhancing the dynamic performance of the overall system.

3.2 Comparison of Couple and Decouple Using Hardware

The discussion in this section begins with a presentation of the results of testing the coupled method on hardware to observe the response characteristics of the system in real conditions. The following section presents the results of testing the decoupled method on hardware to evaluate the effectiveness of separating the interactions between pH and TDS variables in improving control stability. The analysis then continues with a comprehensive comparison between the performance of the two methods, both in simulation and in hardware implementation, to assess the consistency of system behavior and identify the advantages of each approach in controlling pH and TDS.

Analysis of the coupled and decoupled system responses obtained through simulation using the same setpoint, namely pH 6.5 and TDS 550 ppm, was then applied to the device to obtain real-time data. The purpose of this application was to verify the consistency between the simulation results and actual field conditions and to evaluate the performance of pH and TDS control directly. The PID parameter values (K_p, K_i, and K_d) on the device were adjusted to match the values used in the simulation. Hardware testing of the coupled and decoupled methods showed observable differences in performance compared to the simulation results. These differences occurred because the simulation only represented ideal conditions and therefore did not fully describe the dynamics of the real system, which are influenced by sensor noise, actuator delays, process nonlinearities, and environmental uncertainties.

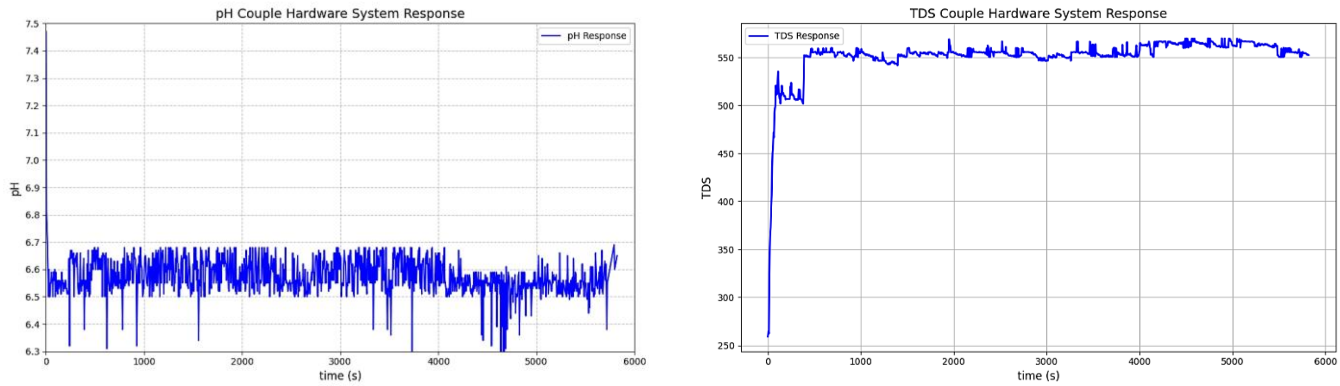

(a) (b)

Figure 7. (a) PH System Response Couple Hardware, (b) TDS System Response Couple Hardware

The results of device testing using the coupled method can be seen in the system response in Figure 7(a). The pH response has a rise time of 18.91 s, indicating that the system requires a relatively long time to reach a condition close to the setpoint. The pH response shows 0% overshoot, indicating that the controller operates in a stable manner without excessive control action or setpoint violation. However, the relatively slow rise time suggests that the pH control loop is still influenced by the slower dynamics of the TDS loop due to loop interaction in the coupled MIMO system. From a physical perspective, the addition of TDS solution and the non-instantaneous mixing dynamics of the nutrient solution introduce gradual disturbances to the pH variable, causing the controller to respond conservatively and resulting in a slower convergence toward steady-state conditions. This validates the theory that cross-coupling increases error propagation between loops, thereby increasing the likelihood of an underdamped transient response [27]. The steady-state error of 0.96% and a settling time of 21 s indicate that the system can maintain stable operation under steady-state conditions. In Figure 7(b), the TDS response has a rise time of 90.95 s and a settling time of 391 s, indicating that the system requires a considerable amount of time to reach the setpoint and stabilize. The cross-coupling effect from the pH loop adds interference, causing the effective time constant of the TDS loop to become significantly greater than its original process characteristics. The overshoot value is 4.61%, and the steady-state error is 1.44%.

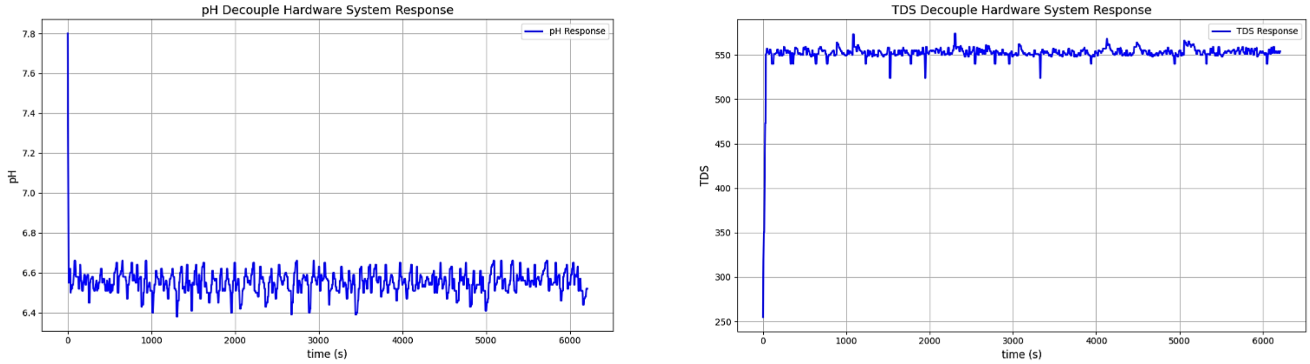

(a) (b)

Figure 8. (a) PH System Response Decouple Hardware, (b) TDS System Response Decouple Hardware

The results of device testing using the decoupled method can be seen in the system response in Figure 8(a). The pH response has a rise time of 8.34 s, indicating that the system reaches a condition close to the setpoint relatively quickly. The pH loop exhibits 0% overshoot, a steady-state error of 0.90%, and a settling time of 11 s. The fast-settling time compared to the coupled method illustrates that the pH loop is no longer disturbed by changes in TDS. The decoupler has eliminated cross-interference, so the dynamics of the pH loop now reflect its intrinsic chemical process dynamics. In Figure 8(b), the TDS response has a rise time of 30.7 s, a settling time of 36 s, and a steady-state error of 0.60%, indicating that the system reaches the setpoint and stabilizes more rapidly. There is a small overshoot of 4.36%. This improvement in response performance occurs because the addition of pH solution no longer alters nutrient concentration, so the TDS controller does not need to correct for disturbance effects propagated from the pH loop. In the hardware implementation, the improved performance achieved with the decoupled control approach demonstrates that interaction compensation remains effective under real operating conditions. Factors such as sensor noise, actuator delay, and non-instantaneous nutrient mixing—commonly encountered in practical hydroponic systems—did not negate the benefits of decoupling. This indicates that the proposed control strategy is robust and suitable for real-time implementation.

3.3 Comparison of Coupled and Decoupled Methods in Simulation and Hardware

Based on the performance evaluation results obtained from both simulation tests and hardware implementation, clear differences in response characteristics are observed between the coupled and decoupled control methods for pH and TDS regulation. Overall, the decoupled method demonstrates superior control performance compared to the coupled approach, particularly in terms of transient response speed and steady-state accuracy. In the simulation results, the decoupled control strategy exhibits more stable and predictable system behavior. Cross-interactions between the pH and TDS control loops are significantly reduced, allowing each controller to operate according to its intrinsic process dynamics. This condition results in faster convergence toward steady-state conditions and reduced oscillatory behavior compared to the coupled method. In contrast, the coupled control approach still shows noticeable inter-loop interactions, which lead to less stable and less predictable system responses. Similar performance improvements are also observed in the hardware implementation. The decoupled method consistently achieves faster transient responses and smaller steady-state errors for both pH and TDS control compared to the coupled method. Although the real system is affected by non-ideal factors such as sensor noise, actuator delays, non-instantaneous nutrient mixing dynamics, and pump nonlinearities, the advantages of interaction compensation remain evident. This indicates that the proposed decoupled control strategy is robust and suitable for real-time implementation in practical hydroponic systems.

The differences between simulation and hardware results are mainly attributed to the ideal assumptions used in the simulation model, including disturbance-free operation, absence of parameter uncertainty, and ideal actuator dynamics. Nevertheless, the consistent performance improvement achieved by the decoupled method in both simulation and real-time experiments confirms that the observed benefits are not merely simulation artifacts but are realizable in physical systems. When compared to previous hydroponic control studies employing data-driven approaches such as Adaptive Network-Based Fuzzy Inference System (ANFIS) and Convolutional Neural Network (CNN), the proposed decoupled PID method offers a distinct advantage for real-time multivariable control applications. While machine learning–based methods often emphasize prediction accuracy, their effectiveness depends heavily on the availability of high-quality training data and substantial computational resources. In contrast, the decoupled PID approach directly enhances control dynamics such as transient response and steady-state regulation while maintaining low computational complexity, making it more suitable for embedded control systems.

These findings are consistent with previous research [28], which reports that decoupling techniques can significantly improve control accuracy and stability in multivariable systems by mitigating inter-loop coupling effects.

From a practical perspective, improved stability in pH and TDS regulation supports more consistent nutrient composition, reduces fluctuations that may interfere with nutrient absorption, and enhances the efficiency of water and nutrient utilization. Therefore, the proposed decoupling-based control strategy represents a non-trivial and practically validated contribution that improves the reliability and performance of real-time hydroponic control systems.

4. Conclusion

The implementation of the pH and TDS control system hardware in hydroponics was successfully carried out using both the coupled and decoupled methods. Simulation results show that the coupled method has a slightly faster rise time and settling time than the decoupled method; however, the decoupled method exhibits lower overshoot. In hardware implementation, the decoupled method is superior, with a pH rise time of 8.34 s, a settling time of 11 s, 0% overshoot, and a steady-state error of 0.90%, while the TDS response has a rise time of 30.7 s, a settling time of 36 s, an overshoot of 4.36%, and a steady-state error of 0.60%. Meanwhile, the coupled method produces a slower response with longer rise time and settling time, as well as a higher steady-state error. This difference occurs because the decoupling method is able to attenuate loop interactions, allowing the system to respond faster and operate more stably. Thus, the decoupling method has been proven to be more effective and responsive in maintaining pH and TDS stability and has strong potential to improve the efficiency and reliability of hydroponic control systems. Control performance can be further enhanced through the application of adaptive or advanced control strategies, such as Model Predictive Control (MPC), to ensure that the system response remains optimal under varying plant growth conditions and environmental disturbances.

References

[1] H. Nirwani and R. Hidayati, “Thermal Comfort for various Altitudes and Land Covers in North Sumatra,” vol. 37, no. 2, pp. 91–98, 202. https://doi.org/10.29244/j.agromet.37.2.91-98

[2] S. R. Giyarsih *et al.*, “Interrelation of urban farming and urbanization : an alternative solution to urban food and environmental problems due to urbanization in Indonesia,” no. January, pp. 1–10, 2024. https://doi.org/10.3389/fbuil.2023.1192130

[3] H. Sirhan, M. Al-ajouz, and R. Al-sa, “Hydroponics as a Sustainable Water-Efficient Agricultural Strategy for Enhancing Resilience and Food Security in the Gaza Strip,” vol. 1, no. 3, pp. 6–20, 2025. https://doi.org/10.63095/NBSEH.25.774983

[4] A. Ullah, S. Aktar, N. Sutar, R. Kabir, and A. Hossain, “Cost Effective Smart Hydroponic Monitoring and Controlling System Using IoT,” *Intell. Control Autom.*, vol. 10, no. 04, pp. 142–154, 2019. https://doi.org/10.4236/ica.2019.104010

[5] F. B. Kelana, N. I. Aulia, P. Studi, T. Pertanian, F. Pertanian, and U. Sriwijaya, “Efektivitas dalam Memantau dan Mengontrol Sistem Hidroponik Apung pada Pertumbuhan Pakcoy Berbasis Sensor TDS Arduino Uno R3,” vol. 19, no. 1, pp. 49–56, 2025. https://doi.org/10.24198/jt.vol19n1.7

[6] H. Sulaiman, A. A. Yusof, and M. K. Mohamed Nor, “Automated Hydroponic Nutrient Dosing System: A Scoping Review of pH and Electrical Conductivity Dosing Frameworks,” *AgriEngineering*, vol. 7, no. 2, pp. 1–23, 2025. https://doi.org/10.3390/agriengineering7020043

[7] D. Adidrana, A. Rahmat, A. Nurhayati, and M. Ramdhani, “Simultaneous Hydroponic Nutrient Control Automation System Based on Internet of Things,” vol. 6, no. March, pp. 124–129, 2022. https://doi.org/10.30630/joiv.6.1.865

[8] J. E. Elektro, D. Yulianto, A. F. Nugraha, F. F. Rahami, and U. A. Dahlan, “Automated Hydroponics System using the Internet of Things,” vol. 8, no. 2, pp. 149–160, 2024. https://doi.org/10.21831/jee.v8i2.76816

[9] N. Surantha and V. Vincentdo, “NFT-Based Hydroponic Automated Control Using Adaptive Network-Based Fuzzy Inference System,” *2022 2nd Int. Conf. Robot. Autom. Artif. Intell. RAAI 2022*, pp. 118–123, 2022. https://doi.org/10.1109/RAAI56146.2022.10092958

[10] Fitriani, Z. Zainuddin, and Syafaruddin, “Nutrition Control System In Nutrient Film Technique (NFT) Hydroponics With Convolutional Neural Network (CNN) Method,” *Proc. - ISMODE 2022 2nd Int. Semin. Mach. Learn. Optim. Data Sci.*, pp. 41–46, 2022. https://doi.org/10.1109/ISMODE56940.2022.10180412

[11] D. L. Methods, “JOURNAL OF ENGINEERING SCIENCES Hydroponic Agriculture with Machine Learning and,” vol. 9, no. 3, pp. 508–519, 2023. https://doi.org/10.30855/gmbd.0705083

[12] K. Jangala, M. Rathaiah, R. Kiranmayi, P. Bharat Kumar, K. Nagabhushanam, and N. Swathi, “Improved Fractional Filter IMC-PID Controller Design for SISO and MIMO Processes,” *2023 5th Int. Conf. Electr. Comput. Commun. Technol. ICECCT 2023*, pp. 1–5, 2023. https://doi.org/10.1109/ICECCT56650.2023.10179712

[13] A. F. Zrigan, A. J. Abougarair, M. K. Elmezughi, and A. M. Almaktoof, “Optimized PID Controller and Generalized Inverted Decoupling Design for MIMO System,” *Proc. 2023 IEEE Int. Conf. Adv. Syst. Emergent Technol. IC_ASET 2023*, pp. 1–6, 2023. https://doi.org/10.1109/IC_ASET58101.2023.10150957

[14] G. Sitaramu, L. Dutta, and D. Kumar Das, “To Design Sigmoid Based PID Controller for Twin Rotor MIMO System,” *2023 2nd IEEE Int. Conf. Meas. Instrumentation, Control Autom. ICMICA 2023*, pp. 1–5, 2024. https://doi.org/10.1109/ICMICA61068.2024.10732610

[15] H. Sukri, A. B. Putra, A. F. Ibadillah, M. Ulum, D. N. Purnamasari, and M. Hardiwansyah, “Automatic Charcoal Briquette Making Machine Tool with PID Control Approach Using Ziegler-Nichols Tuning Method for Energy Efficiency and Productivity,” *Proceeding - IEEE 10th Inf. Technol. Int. Semin. ITIS 2024*, pp. 89–95, 2024. https://doi.org/10.1109/ITIS64716.2024.10845718

[16] A. Dubravic, D. Demirovic, and A. Serifovic-Trbalic, “Optimization of PID Controller Using PSO Algorithm for a First Order Plus Dead Time (FOPDT) Process -A Simulation Study,” *Int. Conf. Electr. Comput. Energy Technol. ICECET 2022*, no. July, pp. 1–4, 2022. https://doi.org/10.1109/ICECET55527.2022.9872631

[17] L. Liu, S. Tian, D. Xue, T. Zhang, Y. Chen, and S. Zhang, “A Review of Industrial MIMO Decoupling Control, Automation and Systems,” *Int. J. Control*, vol. 17, no. X, pp. 1–9, 2019. https://doi.org/10.1007/s12555-018-0367-4

[18] R. Li, Q. Kong, J. Ma, and K. Liang, “Decoupling Control Method of Temperature and Humidity in Long Storage Environment Based on Particle Swarm Optimization PID Algorithm,” *Proc. - 2023 Int. Conf. Adv. Electr. Eng. Comput. Appl. AEECA 2023*, pp. 902–907, 2023. https://doi.org/10.1109/AEECA59734.2023.00164

[19] K. Liu, Y. Liu, F. Song, C. Zhang, W. Li, and Z. Wang, “Data Driven Dynamic Decoupling Control for MIMO Precision Mechatronic Systems,” *Proc. 2024 IEEE 13th Data Driven Control Learn. Syst. Conf. DDCLS 2024*, pp. 1305–1310, 2024. https://doi.org/10.1109/DDCLS61622.2024.10606678

[20] P. Catota-ocapana, C. Minaya-andino, P. Astudillo, and D. Pichoasamin, "Smart Control Models Used for Nutrient Management in Hydroponic Crops : A Systematic Review," vol. 13, no. January, 2025. https://doi.org/10.1109/ACCESS.2025.3526171
[21] F. Wang, Y. Shi, and Y. Chen, "Hierarchical MIMO Decoupling Control for Vehicle Roll and Planar Motions With Control Allocation," vol. 73, no. 1, pp. 494–503, 2024. https://doi.org/10.1109/TVT.2023.3308577
[22] C. G. Proudfoot, "Principles and practice of automatic process control. Carlos A. Smith and Armando B. Corripio," *Automatica*, vol. 23, no. 3, p. 414, 1987. https://doi.org/10.1016/0005-1098(87)90018-5
[23] S. A. Aessa, S. W. Shneen, and M. K. Oudah, "Optimizing PID Controller for Large-Scale MIMO Systems Using Flower Pollination Algorithm," *J. Robot. Control*, vol. 6, no. 2, pp. 553–559, 2025. https://doi.org/10.18196/jrc.v6i2.24409
[24] D. S. Bhandare, N. R. Kulkarni, and M. V. Bakshi, "Linearization of a Coupled tank MIMO system and its validation using MATLAB," *2021 6th Int. Conf. Converg. Technol. I2CT 2021*, pp. 1–5, 2021. https://doi.org/10.1109/I2CT51068.2021.9417875
[25] J. M. Daif-Alkhasraji, S. W. Shneen, and M. Q. Sulttan, "Reduction of Large Scale Linear Dynamic MIMO Systems Using ACO-PID Controller," *Ing. e Investig.*, vol. 44, no. 1, pp. 1–7, 2024. https://doi.org/10.15446/ing.investig.106657
[26] P. Kumar, V. Kumar, and B. Tyagi, "Experimental Validation of PI Controllers and Modelling of DC Servo Motor by FOPDT Model," *PESGRE 2022 - IEEE Int. Conf. "Power Electron. Smart Grid, Renew. Energy,"* pp. 1–5, 2022. https://doi.org/10.1109/PESGRE52268.2022.9715815
[27] M. Science, "Cross-Coupled Dynamics and MPA-Optimized Robust MIMO Control for a Compact Unmanned Underwater Vehicle," 2023. https://doi.org/10.3390/jmse11071411
[28] S. R. Mahapatro and B. Subudhi, "A New H∞Weighted Sensitive Function-Based Robust Multi-Loop PID Controller for a Multi-Variable System," *IEEE Trans. Circuits Syst. II Express Briefs*, vol. 71, no. 3, pp. 1256–1260, 2024. https://doi.org/10.1109/TCSII.2023.3319388